Bistability of Polymers in Pores

Dirk Loomans,* Igor M. Sokolov,† and Alexander Blumen

Theoretische Polymerphysik, Universität Freiburg, Rheinstrasse 12, D-79104 Freiburg i. Br., Germany

Received December 18, 1995; Revised Manuscript Received March 11, 1996[⊗]

ABSTRACT: We consider an ideal chain with fixed ends which passes through a slip-link situated midway on the axis connecting the ends. When the chain is long enough, the system exhibits bistability: in equilibrium the number of segments on the two sides of the slip-link differ.[1] We show that introducing additional geometrical constraints (i.e., having the polymer inside two adjacent boxes connected by a slip-link) changes the situation: The shape of the boxes determines whether the asymmetry persists. For boxes elongated along the axis, the situation is symmetric, whereas for flat boxes, bistability may occur.

1. Introduction

The statistical properties of confined ideal chains (constrained random walks) are of great importance in polymer science; the problem is fundamental in the description of polymers in gels. Although ideal chains seem to be very simple, unexpected results keep on emerging; see the quite recent works by Rieger[1] and by Mansfield.[2] They considered an ideal polymer chain of $2N$ segments whose ends are fixed, say, at the distance $2L_x$. Furthermore, the chain is required to pass through a slip-link situated midway between the ends. It turns out that if L_x is small enough, the entropically most probable situations are asymmetric. Let the number of segments left and right of the slip-link be denoted by N_1 and N_2 in mechanical equilibrium (corresponding to a minimal free energy). For L_x large, one has $N_1 = N_2$, whereas for small L_x, one finds $N_1 \neq N_2$. We denote the latter situation as being bistable; because of symmetry, one may have as well N_2 segments to the left and N_1 segments to the right of the slip-link. We note that the bistable situation occurs only for chains whose ends are pinned (see below and ref 2).

In the present article, we consider a slightly different model in which the ideal chain is confined inside two adjacent boxes connected by a small hole. We show that the existence of the external constraints (the closed walls of the box) changes the behavior of the system strongly. To depict the problem, let us consider two adjacent, identically shaped parallelepipeds connected through a hole located at the center of their common wall; see Figure 1. A polymer occupies both boxes, and the hole serves as a slip-link. The ends of the molecule are pinned on the walls opposite to the hole. As we now proceed to show, the occurrence of bistability for long molecules is governed by the aspect ratio (ratio of length to width) of the parallelepiped: in strongly elongated boxes, only symmetric (monostable) states are possible.

Our study is motivated by the fact that although the slip-link model is of common use for polymers in gels and in porous media,[3,4] there are many instances in which the restricted geometry dictated by the pores is significant. As an example, let us consider the lakes−straits model for DNA gel electrophoresis.[5] In this model, the DNA molecule, described by a random-flight chain, lies in a series of pores (lakes) connected by openings (straits). As we have shown elsewhere,[6,7] taking into account the boundaries of the pores greatly affects the results of the model. Electrophoresis is of great importance in applications and requires the understanding of basic properties of polymers in restricted geometries. We note that bistability effects can be found in many systems, such as the problems of minimal paths and surfaces (i.e., soaps[8]).

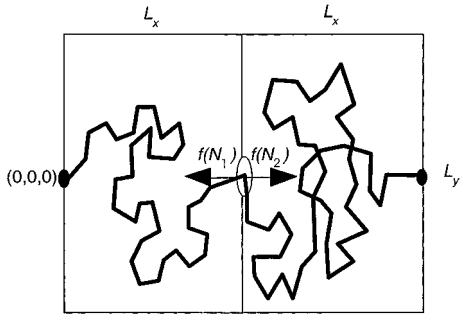

Figure 1. A freely-jointed polymer in two boxes (pores) connected by a slip-link.

Our considerations parallel those of Rieger[1] and Mansfield[2] but make explicit use of tension forces. This representation is, of course, in line with the former works but is closer to intuition, since it renders clear the mechanical nature of the equilibrium state. We consider here only the most probable configurations of a macromolecule confined inside *two* boxes; the generalization to situations involving many boxes can be performed along the lines of ref 2.

2. Bistability in the Simple Slip-Link Model

We start from a situation in which the only restrictions imposed on the chain are the fixed ends and the slip-link. In equilibrium the entropic tension on the fragment on the left side of the slip-link equals that on the right side:

$$f(N_1) = f(N_2) \tag{1}$$

Furthermore, there is the evident constraint

$$N_1 + N_2 = 2N \tag{2}$$

In a bistable situation one has $N_1 \neq N_2$, whereas the symmetric case has the (trivial) solution $N_1 = N_2 = N$. The entropic tension on a chain fragment of n segments is[2,5]

† Also at P. N. Lebedev Physical Institute of the Academy of Sciences of Russia, Leninsky Prospekt 53, Moscow 117924, Russia.

[⊗] Abstract published in *Advance ACS Abstracts,* May 15, 1996.

S0024-9297(95)01862-6 CCC: $12.00

$$f(n) = \frac{3k_BT}{2a}\left[\frac{1}{n} - \left(\frac{L_x}{an}\right)^2\right] \tag{3}$$

(see also section 3) with a being the segment length. Positive values of $f(n)$ represent forces acting to lower the number of chain segments between the fixed end and the slip-link. The sign convention in eq 3 is as in ref 2 and is opposite to the one of ref 5. The tension, eq 3, is negative for small n, goes through zero at $n = n_0 = (L_x/a)^2$, attains a maximum at $n = n_c = 2(L_x/a)^2$, and then tends to zero for $n \to \infty$. We hasten to note that eq 3 may be written in a dimensionless form by introducing $\nu = na^2/L_x^2$ and $\varphi(\nu) = f(n)L_x^2/(ak_BT)$:

$$\varphi(\nu) = \frac{3}{2}(\nu^{-1} - \nu^{-2}) \tag{4}$$

Using eq 4, one can rewrite eq 1 in the form

$$\varphi(\xi_1) = \varphi(2\xi - \xi_1) \tag{5}$$

with $\xi = Na^2/L_x^2$ and $\xi_1 = N_1a^2/L_x^2$. In Figure 2, we present $\varphi(\xi_1)$, depicted as a solid line. Furthermore, we also give $\varphi(2\xi - \xi_1)$ for $\xi = 1$ (dotted line) and for $\xi = {}^5/_2$ (dashed line). Note that the last two curves are simply shifted with respect to each other. The intersections of these curves with $\varphi(\xi_1)$ determine the solutions of eq 5. One sees by inspection of Figure 2 that for $\xi = 1$ only one solution exists, whereas for $\xi = {}^5/_2$ there are three solutions, two stable and one unstable. Furthermore, it is evident that bistability is related to the position $\xi_c = n_ca^2/L_x^2 = 2$ of the maximum of φ: bistable situations occur for $\xi > \xi_c$. In this case, eq 5 has three solutions:

$$\xi_1 = \xi \quad \text{and} \quad \xi_1 = \xi \pm (\xi^2 - \xi)^{1/2} \tag{6}$$

the first being symmetric and the other two being asymmetric. In the opposite case, $\xi < \xi_c$, only one solution, $\xi_1 = \xi$, exists. Note that the occurrence of bistability is related to the fact that $\varphi(\xi)$ shows a maximum; otherwise only a symmetric solution is possible.

Thus for a polymer whose ends are fixed the free energy in the presence of a slip-link displays one or two clear-cut minimal points. If, however, the ends of the polymer are free, the free energy shows no such extrema[2] and the dynamics of the chain is dictated by the fluctuations.

3. Bistability under Geometrical Constraints

We start by evaluating the tension on an ideal polymer chain confined in a box. For this we detail somewhat the derivation in order to render clear the role of the initial and of the boundary conditions. The calculation parallels that of the pressure exercised by a polymer on the walls of a box:[9,10] both calculations are based on the Green's function of the corresponding diffusion equation.

Let L_x be the length of the box along the main axis and L_y and L_z the width and the height of the box, ordered so that $L_y \geq L_z$; we denote the longitudinal aspect ratio by $\zeta = L_y/L_x$ and the transversal aspect ratio by $\eta = L_z/L_y$ (note that $0 < \eta \leq 1$). Furthermore, the ends B and F of the chain lie on the x-axis and have the coordinates (0,0,0) and (L_x,0,0). The segment length is again a. We model the ideal chain as a simple random walk on a simple cubic (sc) lattice; see Figure 3

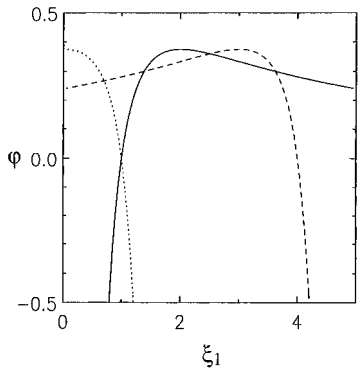

Figure 2. Plot of $\varphi(\xi_1)$, eq 4 as a solid line. Also depicted is $\varphi(2\xi - \xi_1)$ for $\xi = 1$ (dotted line) and for $\xi = 5/2$ (dashed line); see text for details.

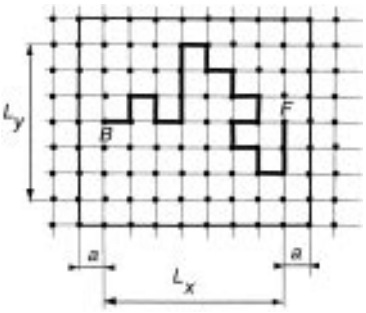

Figure 3. Polymer in a box, modeled as a random walk on a lattice.

for the projection on the xy space. For L_x/a even (odd), all the allowed walks have n even (odd) steps.

The tension $f(n)$ on a fragment of n segments can be calculated through the work necessary to pull out from the box two segments of the fragment and equals

$$f(n) = \frac{F(n+1) - F(n-1) - k_BT \ln C}{2a} \tag{7}$$

In eq 7 $F(n)$ is the free energy of the fragment considered, k_B is the Boltzmann constant, and C is the coordination number (number of nearest neighbors of a site; e.g., $C = 6$ for sc); see ref 7 for a discussion. The free energy $F(n)$ is given by

$$F(n) = -k_BT \ln W(n) \tag{8}$$

where $W(n)$ is the number of different configurations (walks of n steps) leading from the starting point B to the exit slip-link F. For a closed box, the allowed random walks never cross the walls, i.e., in Figure 3 never touch the next layer of sites (boundary); this corresponds to an infinite repulsive potential for the boundary sites. Therefore the number $W(n)$ of possible configurations is equal to the number $Z_n(F,B)$ of walks of n steps beginning at point B and ending at point F (see Figure 3).

Now $W(n) = Z_n(F,B)$ can be calculated recursively by noting that $Z_n(i,B)$, the number of walks of n steps ending at a given site i, is equal to the sum of the numbers of walks of length $n - 1$ ending at the nearest neighbors of i:

$$Z_n(i,B) = \sum_{j \in nn} Z_{n-1}(j,B) \tag{9}$$

In eq 9 the summation goes over all nearest neighbors of i. There are no walks leading from points inside the

box to the boundary points, from which the boundary condition $Z|_{\text{boundary}} = 0$ follows. The initial condition is $Z_0(i,B) = \delta_{i,B}$. Equation 9 is then the basis both for the numerical evaluation of the forces using the cellular automaton algorithm (see ref 7) and also for the further analytical considerations.

Setting $G_n(j,B) = Z_n(j,B)/C^n$, one has from eq 9

$$G_n(j,B) = C^{-1} \sum_{i \in nn} G_{n-1}(i,B) \tag{10}$$

Rewriting eq 10 in the form

$$G_n(j,B) - G_{n-1}(j,B) = C^{-1} \sum_{i \in nn} \{G_{n-1}(i,B) - G_{n-1}(j,B)\} \tag{11}$$

and reverting from the discrete scheme to the continuum ($i \rightarrow \mathbf{r}$, $B \rightarrow \mathbf{b} = (0,0,0)$) leads in well-known fashion to the diffusion equation for the Green's function $G(\mathbf{r},\mathbf{b};n)$:

$$\frac{\partial G(\mathbf{r},\mathbf{b};n)}{\partial n} = \frac{a^2}{6} \Delta_{\mathbf{r}} G(\mathbf{r},\mathbf{b};n) \tag{12}$$

where $\Delta_{\mathbf{r}}$ is the Laplace operator. The initial condition is $G(\mathbf{r},\mathbf{b};0) = \delta(\mathbf{r}-\mathbf{b})$, and the walls are taken into account through the (absorbing) boundary condition $G(\mathbf{r},\mathbf{b};n)|_{\text{boundary}} \equiv 0$.

According to eqs 8−10 (with $F \rightarrow \mathbf{f} = (L_x,0,0)$), the free energy of a chain in a box is

$$F(n) = -k_B T(\ln G(\mathbf{f},\mathbf{b};n) + n \ln C) \tag{13}$$

from which the tension follows from eq 7:

$$f(n) = -\frac{k_B T}{a} \frac{\partial}{\partial n} \ln G(\mathbf{f},\mathbf{b};n) \tag{14}$$

The case of a nonconfined chain passing through a slip-link (the situation considered by Rieger[1] and Mansfield[2]) is given by the Green's function of eq 12 in free space:

$$G(\mathbf{f},\mathbf{b};n) = \left(\frac{2}{3}\pi a^2 n\right)^{-3/2} \exp\left(-\frac{3L_x^2}{2a^2 n}\right) \tag{15}$$

where we used that $(\mathbf{f} - \mathbf{b})^2 = L_x^2$. From eqs 14 and 15, the standard form for the tension, eq 3, immediately follows.

We now evaluate the tension on a chain fragment in a box. The Green's function G for a macromolecule in a box was considered in ref 9; G is constructed from the eigenfunctions of eq 12, which satisfy the boundary conditions and thus vanish at $x = -a$, $x = L_x + a$, $y = \pm(L_y/2 + a)$, and $z = \pm(L_z/2 + a)$. Parallel to eq 2.8 of ref 9, one obtains

$$G(\mathbf{r},\mathbf{b};n) = \left(\frac{8}{XYZ}\right) \sum_{k_x=1}^{\infty} \sum_{k_y=0}^{\infty} \sum_{k_z=0}^{\infty} \sin\frac{\pi a k_x}{X} \sin\frac{\pi k_x (x+a)}{X} \cos\frac{\pi(2k_y+1)y}{Y} \cos\frac{\pi(2k_z+1)z}{Z} \exp\left(-\frac{\pi^2 a^2}{6}\left(\frac{k_x^2}{X^2} + \frac{(2k_y+1)^2}{Y^2} + \frac{(2k_z+1)^2}{Z^2}\right)n\right) \tag{16}$$

with $X = L_x + 2a$, $Y = L_y + 2a$, and $Z = L_z + 2a$. Inside the box, eq 16 satisfies the condition $G(\mathbf{r},\mathbf{b};0) = \delta(\mathbf{r}-\mathbf{b})$, as can be verified by summation of the series for $n = 0$.

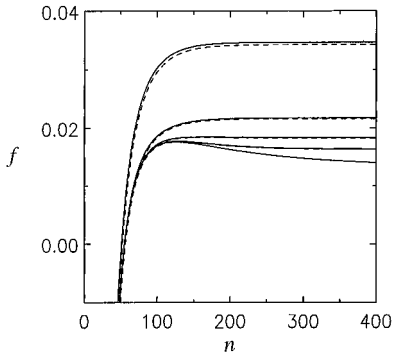

Figure 4. Force $f(n)$ in units of $(ak_BT)/L_x^2$, calculated for pores with $L_x = 10a$ and square cross-section with side length $L_y = L_z = L$; the latter values are $10a$, $16a$, $20a$, $24a$, and $40a$ from top to bottom. The dashed lines correspond to the continuous expression, eq 20, and the solid ones are obtained from an exact enumeration method on a sc lattice; see text for details.

Note that in eq 16 the triple series decouples into a product of three single series; for $G(\mathbf{r},\mathbf{b};n)$ we have

$$G(\mathbf{f},\mathbf{b};n) = g_x(n,X)\, g_\perp(n,Y)\, g_\perp(n,Z) \tag{17}$$

In eq 17 the functions $g_x(n,L)$ and $g_\perp(n,L)$ (with $L = X$, Y, or Z) are given by

$$g_x(n,L) = \frac{2}{L} \sum_{k=1}^{\infty} (-1)^{k+1} \sin^2\frac{\pi a k}{L} \exp\left(-\frac{\pi^2 a^2 k^2}{6L^2} n\right) \tag{18}$$

and

$$g_\perp(n,L) = \frac{2}{L} \sum_{k=0}^{\infty} \exp\left(-\frac{\pi^2 a^2 (2k+1)^2}{6L^2} n\right) \tag{19}$$

The tension can be now evaluated according to eq 14:

$$f(n) = -\frac{k_B T}{a} \frac{\partial}{\partial n} [\ln g_x(n,X) + \ln g_\perp(n,Y) + \ln g_\perp(n,Z)] \tag{20}$$

with use of eqs 18 and 19.

As we proceed to show, the series in eq 19 converge rapidly for $n > L^2/a^2$, n values which are of most interest; essentially one has to sum the first $L/(an^{1/2})$ terms of the series. We checked this by comparing the results of eq 20 to the numerically determined force; the latter starts from the exact evaluation of $W(n)$ via eq 9 through a cellular automaton algorithm (see ref 7) and uses eqs 7 and 8. In Figure 4 we present the results for pores of square cross-section ($L_x = L_y = L$) while the value of L_x is fixed at $L_x = 10a$. From Figure 4 one readily infers that eq 20 is very accurate even for L values as small as $10a$; moreover, the accuracy of the continuous expression improves very fast for increasing L. From Figure 4 one sees that $f(n)$ exhibits a clear maximum for flat pores ($L_y = L_z \gg L_x$); the maximum gets less pronounced and eventually disappears as $L_y = L_z$ approaches L. This finding is, of course, confirmed by inspecting the numerical values of f (not given here). We have found no numerical evidence for other types of behavior, e.g., other extrema.

As pointed out in section 2, the appearance of a maximum is related to bistability. We now turn to the question of establishing analytically conditions under

which $f(n)$ shows an extremum; for this we investigate the behavior of $f(n)$ for n large. Now the force on a very long chain ($n \to \infty$) is given by the term with $k_x = 1$; $k_y = k_z = 0$, i.e., by the lowest eigenvalue in eq 16. Using eqs 16−19, one finds

$$f_\infty = \lim_{n\to\infty} f(n) = \frac{k_B T a}{6}\left(\frac{1}{X^2} + \frac{1}{Y^2} + \frac{1}{Z^2}\right) \qquad (21)$$

where $X = L_x + 2a$, $Y = L_y + 2a$, and $Z = L_z + 2a$. Now $f(n)$ can approach f_∞ either from below (in this case $f(n)$ is monotonous and has no extrema) or from above (then $f(n)$ exhibits a maximum). To see what type of behavior really occurs, it is sufficient to consider whether, for a large but finite value of n, f is larger or smaller than f_∞. To check this, we simply take into account the next terms in the expansion of eq 16, namely the ones corresponding to (k_x,k_y,k_z) being (2,0,0), (1,1,0), or (1,0,1). In this case, we have

$$f(n) - f_\infty \cong \frac{\pi^2 a^2 f_\infty}{6}\left[-\cos^2\frac{\pi a}{X^2}\left(\frac{4}{X^2} + \frac{1}{Y^2} + \frac{1}{Z^2}\right)\right.$$
$$\exp\left(-\frac{\pi^2 a^2}{2}\frac{n}{X^2}\right) + \left(\frac{1}{X^2} + \frac{9}{Y^2} + \frac{1}{Z^2}\right)\exp\left(-\frac{4\pi^2 a^2}{3}\frac{n}{Y^2}\right) +$$
$$\left.\left(\frac{1}{X^2} + \frac{1}{Y^2} + \frac{9}{Z^2}\right)\exp\left(-\frac{4\pi^2 a^2}{3}\frac{n}{Z^2}\right)\right] \qquad (22)$$

Note that the negative contributions comes from the first term in brackets, whereas the other two terms are positive. For $n \to \infty$ the relative importance of these terms does not depend on their prefactors, but only on the exponents. Thus, $f(n) - f_\infty$ is negative when the first term prevails, and positive otherwise. Note that asymptotically due to our convention, $L_y > L_z$, the third term can never get larger than the second one. Hence, in our qualitative description we find no maximum for $Y/X < (8/3)^{1/2} \approx 1.633$, independently of the second transverse length. Note that for large pores $\zeta \approx Y/X$, so that the existence of bistability is governed by ζ.

We conclude this section by emphasizing that the form of the box is extremely important for bistability, which does not take place for elongated boxes; the situation for a simple slip-link corresponds to a box with very large transversal dimensions.

4. The Polymer Inside Two Boxes

We now turn to the consideration of a polymer confined in two boxes. As we already mentioned, the system is in mechanical equilibrium if the entropic tension on the left-side fragment equals the tension on the right-side fragment; see eqs 1 and 2. Bistability corresponds to a solution with $N_1 \neq N_2$ and is connected with the appearance of a maximum of $f(n)$.

For elongated boxes $f(n)$ is monotonous, whereas for flat boxes $f(n)$ displays a maximum. If bistability is possible, its onset is characterized by a critical number of segments N_c, which is related to the position of the maximum of $f(n)$. Parallel to the case of a slip-link, we introduce the parameter $\xi = na^2/L_x^2$ and characterize the transition to bistability by the critical value $\xi_c = N_c a^2/L_x^2$, where N_c is the value of n for which $f(n)$ attains its maximum. This value can readily be evaluated numerically using the analytical forms for $f(n)$ discussed above.

Both the analytical expression and the numerical evaluation of the force show that in general ξ_c takes values of order unity. Therefore for $L_x \gg a$ one may set $\sin^2(\pi a k_x/X) \approx (\pi a k_x/X)^2$ in eq 18. Moreover, for large pores one can also neglect the differences between X, Y, and Z and L_x, L_y, and L_z, respectively. The dependence of $f(n)$ on n and on the side lengths of the box reduces then to a dependence on the three dimensionless variables ξ, ζ, and η. Parallel to the case of a slip-link only, one may set

$$f(n) = \frac{a k_B T}{L_x^2}\varphi_{\zeta,\eta}(\xi) \qquad (23)$$

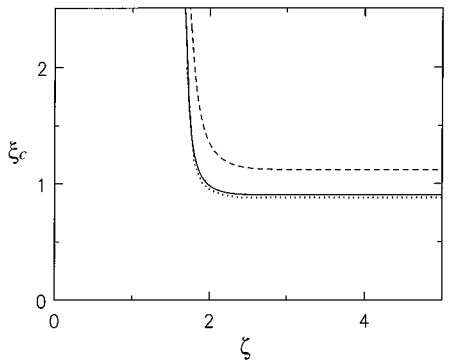

Figure 5. Plot of ξ_c as a function of ζ for various values of η. The bistable situation is obeyed for $\xi > \xi_c$. Displayed are the cases $\eta = 1$ for $L_x = 10a$ (dotted line), $\eta = 1$ for $L_x = 30a$ (solid line), and the limiting case $\eta \to 0$ (dashed line).

In Figure 5 we present ξ_c as a function of ζ for various values of η. We show first the curves obtained for $\eta = 1$, by using for the box $L_x = 10a$ (dotted line) and also $L_x = 30a$ (solid line). The curves practically coincide, which shows that the scaling implied by eq 23 is indeed, for $\eta = 1$, well obeyed. Second, we show in Figure 5 the curve for $\eta \to 0$ (dashed line), a situation which describes an essentially two-dimensional system. Due to our convention for η, one has $0 < \eta \leq 1$; i.e., the region between the curves of Figure 5 covers the whole physical range of interest. From the shape of the curves, we infer that η does not influence their form strongly; for smaller η, the curves are mainly shifted as a whole to higher values of ξ_c.

As a final remark, we note that although the bistability studied here is of importance, for large pores the maxima of the forces considered are so flat that many other factors (friction in the slip-link, external fluctuating forces, etc.) can destroy the effects discussed and may give rise to additional types of behavior.

5. Conclusions

We considered the equilibrium (most probable) configuration of a chain in two similar adjacent boxes connected by a small hole (slip-link). We have shown that the behavior of the macromolecule is strongly influenced by the geometry of the boxes. For elongated boxes, only a symmetrical distribution of segments between boxes is possible, whereas for flat boxes, asymmetrical distributions can occur if the number of segments is large enough. Furthermore, the number of segments necessary for the onset of bistability depends on the aspect ratios of the boxes.

Acknowledgment. The authors thank J. Rieger for drawing their attention to this problem and C. Disch for fruitful discussions. This work was supported by the Deutsche Forschungsgemeinschaft (SFB 60), by the

Fonds der Chemischen Industrie, by EC Grant CHRX-CT93-0354, and by a PROCOPE grant, administrated by the DAAD.

References and Notes

(1) Rieger, J. *Macromolecules* **1989**, *22*, 4540.
(2) Mansfield, M. *Macromolecules* **1991**, *24*, 3395.
(3) Doi, M.; Edwards, S. F. *J. Chem. Soc., Farraday Trans. 2* **1978**, *74*, 1802.
(4) Sommer, J. U. *J. Chem. Phys.* **1992**, *97*, 5777.
(5) Zimm, B. H. *J. Chem. Phys.* **1991**, *94*, 2187.
(6) Loomans, D.; Blumen, A. *Macromol. Symp.* **1994**, *81*, 101.
(7) Loomans, D.; Sokolov, I. M.; Blumen, A. *Macromol. Theory Simul.* **1995**, *4*, 145.
(8) Isenberg, C. *The Science of Soap Films and Soap Bubbles*; Dover Publications: New York, 1992.
(9) Edwards, S. F.; Freed, K. F. *J. Phys. A* **1969**, *2*, 145.
(10) Collins, R.; Wragg, A. *J. Phys. A* **1969**, *2*, 151.

MA9518621